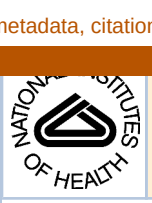

Published in final edited form as:
Development. 2005 February ; 132(3): 553–563.

Tbx5 and *Tbx20* act synergistically to control vertebrate heart morphogenesis

Daniel D. Brown[1,2], **Shauna N. Martz**[1], **Olav Binder**[1], **Sarah C. Goetz**[1,2], **Brenda M. J. Price**[3], **Jim C. Smith**[3], and **Frank L. Conlon**[1,2,*]

1 *Department of Genetics, Fordham Hall, UNC-Chapel Hill, Chapel Hill, NC 27599-3280, USA*

2 *Department of Biology, Fordham Hall, UNC-Chapel Hill, Chapel Hill, NC 27599-3280, USA*

3 *Wellcome Trust/Cancer Research UK Gurdon Institute of Cancer and Developmental Biology and Department of Zoology, University of Cambridge, Tennis Court Road, Cambridge CB2 1QR, UK*

Summary

Members of the T-box family of proteins play a fundamental role in patterning the developing vertebrate heart; however, the precise cellular requirements for any one family member and the mechanism by which individual T-box genes function remains largely unknown. In this study, we have investigated the cellular and molecular relationship between two T-box genes, *Tbx5* and *Tbx20*. We demonstrate that blocking *Tbx5* or *Tbx20* produces phenotypes that display a high degree of similarity, as judged by overall gross morphology, molecular marker analysis and cardiac physiology, implying that the two genes are required for and have non-redundant functions in early heart development. In addition, we demonstrate that although co-expressed, *Tbx5* and *Tbx20* are not dependent on the expression of one another, but rather have a synergistic role during early heart development. Consistent with this proposal, we show that TBX5 and TBX20 can physically interact and map the interaction domains, and we show a cellular interaction for the two proteins in cardiac development, thus providing the first evidence for direct interaction between members of the T-box gene family.

Keywords

Tbx5; *Tbx20*; T-Box; T-domain; Cardiogenesis; Cardiac; Heart; Development; Xenopus laevis

Introduction

The vertebrate heart constitutes the earliest functional organ in the developing embryo and about 1% of all live births exhibit congenital heart disease (Hoffman, 1995a; Hoffman, 1995b; Payne et al., 1995). It is becoming increasingly clear that a complex molecular regulatory network is required to initiate and complete the formation of a functional heart. The proteins implicated in this process include a number of transcription factors from a range of transcription factor families, including the T-box, basic helix-loop-helix homeodomain, zinc finger and MADS domain families (Cripps and Olson, 2002; Harvey, 2002; Zaffran and Frasch, 2002).

The T-box family of transcription factors is a large family of proteins involved in determining early cell fate decisions and controlling differentiation and organogenesis. Two sets of clinical

*Author for correspondence (e-mail: frank_conlon@med.unc.edu).

Supplementary material

Supplementary material for this article is available at http://dev.biologists.org/cgi/content/full/132/3/553/DC1

data have provided direct evidence for the involvement of T-box genes in human heart development (Packham and Brook, 2003; Ryan and Chin, 2003). Deletions of *Tbx1* have been found in individuals with DiGeorge syndrome (Baldini, 2004; Chieffo et al., 1997; Yagi et al., 2003), and mutations in *Tbx5* are associated with Holt-Oram Syndrome (HOS), a congenital heart disease characterized by defects in heart formation and upper limb development (Basson et al., 1997; Li et al., 1997). Clinical studies of individuals with HOS have demonstrated a fundamental role for *Tbx5* in heart development. HOS is a highly penetrant autosomal dominant condition associated with skeletal and cardiac malformations (Newbury-Ecob et al., 1996). Individuals with HOS often carry mutations within the coding region of the T-box transcription factor *Tbx5* (Basson et al., 1997; Basson et al., 1999; Benson et al., 1996; Li et al., 1997). The role of *Tbx5* in heart development, and in the HOS disease state, is further supported by recent gene-targeting experiments in mouse. These studies demonstrate that mice heterozygous for mutations in *Tbx5* display many of the phenotypic abnormalities of individuals with HOS (Bruneau et al., 2001) and show that TBX5 is required for growth and differentiation of the left ventricle and atria as well as for proper development of the cardiac conduction system (Moskowitz et al., 2004). Similar defects are seen in the zebrafish *tbx5* mutant *heartstrings*, suggesting that the expression and function of TBX5 is conserved throughout vertebrate evolution (Garrity et al., 2002).

Previously, we have described the cloning and expression of the *Xenopus laevis* (*X. laevis*) *Tbx20* ortholog, *Tbx20* (Brown et al., 2003). Studies of *Tbx20* have demonstrated that, along with *Tbx5*, *Tbx20* is one of the first genes expressed in the vertebrate cardiac lineage. Moreover, *Tbx20* is expressed at the same time and in many of the same regions of the heart that also express the heart markers *Tbx5*, *Nkx2-5* and *Gata4* (Horb and Thomsen, 1999; Laverriere et al., 1994; Tonissen et al., 1994).

Despite our knowledge of the expression pattern of *Tbx20*, little is known of *Tbx20* function in heart development. In the zebrafish, it has recently been observed that eliminating endogenous TBX20 (HrT) via morpholinos leads to cardiac defects (Szeto et al., 2002). Specifically, TBX20 knockdown in zebrafish leads to dysmorphic hearts and a loss of blood circulation. The morphological defects are not apparent until the cardiac looping stage, despite high levels of *Tbx20* during the earlier stages of specification and development, suggesting that other T-box genes may act redundantly with *Tbx20* during early heart development.

In this study we investigate the cellular and molecular relationship between *Tbx5* and *Tbx20* in *X. laevis*. We show that the phenotypes of knocking down TBX5 and TBX20 are highly similar, with embryos derived from either *Tbx5* or *Tbx20* morpholino injections displaying profound morphological defects, including pericardial edema, reduced cardiac mass and loss of circulation. In addition, we show that the morphological phenotype is not a reflection of alterations in the specification, commitment or differentiation of cardiac tissue. Thus, in addition to sharing a number of molecular properties, we show that *Tbx5* and *Tbx20* function in a non-redundant fashion and are essential for cardiac morphogenesis. However, despite the similarities in phenotype and shared molecular properties, *Tbx5* and *Tbx20* also have independent roles in heart development.

Given the similarity in TBX5 and TBX20 morphant phenotypes, we investigated the pathways by which *Tbx5* and *Tbx20* function. We show that TBX5 and TBX20 do not function in a linear pathway (i.e. *Tbx20* does not act downstream of *Tbx5*, and vice versa), but rather imply a synergistic role for these two proteins during early heart development. Consistent with this proposal, we show that TBX5 and TBX20 can physically interact, map the interaction domains, and show an interaction for the two proteins in cardiac development, therefore providing the first evidence for interaction between members of the T-box gene family.

Materials and methods

DNA constructs

XANF was generously provided by Paul Krieg (p*XANF*) (Small and Krieg, 2000) and the *cardiac troponin I* (p*XTnIc*) plasmid was generously provided by Tim Mohun (Logan and Mohun, 1993). *Nkx*2-5 was cloned by degenerate PCR from a ventral-anterior *X. laevis* cDNA library (generous gift of Tim Mohun). Sequence analysis revealed that the clone shows extensive homology to a partial sequence of the second *X. laevis* allele of *Nkx2-5* (Accession Number, AF283102). The clone is predicted to be full length and in vitro translation of the protein gave a band of the correct size. The clone is referred to as pCRNkx-2.5B (Accession Number, AY644403). To construct the pBS-*Nkx2-5* hybridization probe, *Nkx2-5* was subcloned into pBLUESCRIPT II KS+. All other plasmids and construction information available on request.

Transient transfections

293T cells were plated at 1×10^6 cells/well in six-well tissue culture plates 24 hours prior to transfection. Plasmids used in transients are: the *Nppa* promoter-luciferase reporter (Bruneau et al., 2001; Hiroi et al., 2001), p*Tbx5*-V5, p*Tbx20*-V5, pCMV-*LacZ* and pBS/KS. The amount of luciferase reporter plasmid DNA was kept constant at 100 ng for *Tbx5*, while titering in *Tbx20* (25–100 ng). Expression vector plasmid DNA was kept constant at 100 ng total and 50 ng of *lacZ* reporter plasmid was used. Total amount of DNA was kept constant at 2 μg and transfected using Lipofectamine 2000 (Invitrogen). Plasmid DNA was diluted in OPTI-MEM (GibcoBRL) and complexes were allowed to form for 25 minutes at room temperature and added to each well. Forty-eight hours post-transfection, cells were harvested using M-PER (Pierce) with gentle shaking. Luciferase activity was normalized to β-galactosidase activity. All assays were carried out three independent times in triplicate. Results were plotted using normalized Relative Luciferase Units (RLUs).

Nuclear localization

NIH/3T3 cells were seeded in chamber slides at 6×10^3 cells/chamber 24 hours prior to transfection. Cells were transfected with 187.5 ng p*Tbx20*-V5 or p*Tbx5*-V5 per chamber using 1.25 μl Polyfect (QIAgen) transfection reagent according to manufacturer's protocol. At 48 hours, cells were washed twice with PBS and fixed in MEMFA for 1 hour (2 ml 10×MEM, 2 ml formaldehyde, 16 ml H_2O) at 4°C. Cells were washed twice with PBST (PBS + 0.1% Triton), blocked in PBST + 10% fetal bovine serum for 1 hour at 4°C, incubated at 4°C overnight with anti-V5 (Invitrogen) diluted 1:1000 in PBST+Serum. Cells were washed three times, blocked for 1 hour, then incubated for 1 hour at room temperature with goat anti-mouse Cy2 (Jackson ImmunoResearch) diluted 1:200 in PBST+Serum. This process was repeated using anti-phosphotyrosine (Upstate Biotechnology) as primary antibody to visualize the cytoplasmic compartment and goat anti-mouse Cy3 (Jackson ImmunoResearch) secondary antibody. Cells were washed three times, coverslipped and analyzed by confocal microscopy on a Zeiss LSM 410.

Embryo injections

Preparation and injection of *X. laevis* embryos was carried out as previously described (Wilson and Hemmati-Brivanlou, 1995). Embryos were staged according to Nieuwkoop and Faber (Nieuwkoop and Faber, 1967). Two antisense morpholino oligonucleotides each were designed against the *Tbx5* and *Tbx20* 5′UTRs and start sites. Morpholinos were obtained from Gene Tools, LLC. with the following sequences: Tbx20-MO1, 5′AAT CCA CTT CCA AGG GCA GTT GCT T 3′; Tbx20-MO2, 5′GTT TGG GAG AAG GAG TGT ATT CCA T 3′; Tbx5-MO1, 5′TTA GGA AAG TGT CTC TGG TGT TGC C 3′; Tbx5-MO2, 5′CAT AAG CCT CCT CTG

TGT CCG CCA T 3′; and control MO, 5′CCT CTT ACC TCA GTT ACA ATT TAT A 3′. The human β-globin splice-mutant standard control morpholino from Gene Tools was used as control. Equal amounts of both Tbx5 morpholinos were used in all injections. This combination is referred to in the text and figures as 'TBX5MO'. *Tbx20* morpholinos were also injected in combination, and referred to as 'TBX20MO'. TBX5MO was injected at the optimal (40 ng) or suboptimal (20 ng) doses, and TBX20MO was injected at the optimal (80 ng) or suboptimal (40 ng) doses. 'Optimal dose' is defined as the dose empirically found to be efficient at blocking protein translation both in vitro and in vivo, and inducing a cardiac phenotype in nearly 100% of injected embryos, while 'suboptimal dose' refers to the dose empirically found to be below the threshold of the full cardiac phenotype-inducing dose.

Whole-mount RNA in situ hybridization

Whole-mount in situ hybridization was performed as previously described (Harland, 1991). Embryos were cleared using 2:1 benzyl benzoate/benzyl alcohol (Sigma) (Figs 5 and 9).

Immunohistochemistry

Embryos were collected and fixed for 2 hours at 4°C in 4% paraformaldehyde and rinsed in PBS, incubated overnight in 30% sucrose in PBS at 4°C, mounted in OCT cryosectioning medium (Tissue Tek) and snap frozen. Cryostat sections (14 μm) sections were rinsed with wash buffer (PBS, 1% Triton, 1% serum), incubated at 4°C overnight with anti-tropomyosin (1:50; Developmental Studies Hybridoma Bank) (Kolker et al., 2000), and phalloidin conjugated to Alexa 488 flourophore (Molecular Probes). Sections were then rinsed with wash buffer and incubated with anti-mouse Cy3-conjugated secondary antibody (1:200; Sigma). Sections were rinsed and incubated for 20 minutes at room temperature with DAPI, cover slipped and visualized on a Zeiss LSM410 confocal microscope.

Translation inhibition by morpholinos

In vitro translations were performed using TNT Coupled Reticulocyte Lysate System (Promega) following the manufacturer's protocol. We have recently demonstrated that *X. laevis* SHP-2 is uniformly expressed throughout early development (Y. Langdon and F.L.C., unpublished) and anti-PTP1D/SHP2 primary antibody was used at 1:2500 (Transduction Laboratories) as a loading control with peroxidase-conjugated AffiniPure donkey anti-mouse (H+L) 2° antibody (1:10,000). V5-tagged proteins were probed with anti-V5 primary antibody (Invitrogen) at 1:5000 dilution, and peroxidase-conjugated AffiniPure Donkey anti-mouse (H +L) secondary antibody (Jackson ImmunoResearch Laboratories) at 1:10,000 dilution. For in vivo translation analyses, embryos were injected with MOs and mRNA at the one-cell stage and animal caps cut at stage 8. At sibling stage 10, 10 animal caps per treatment were collected and lysed in 100 μl of lysis buffer: 200 mM NaCl, 20 mM NaF, 50 mM Tris (pH 7.5), 5 mM EDTA, 1% IGEPAL, 1% Triton X-100 (Sigma), Complete EDTA-free Protease Inhibitor (Roche). Lysates were resolved on 12% SDS-PAGE gels, and visualization was carried out using Western Lightning Chemiluminescence Reagent Plus (PerkinElmer Life Sciences).

Glutathione-S-transferase pull-down assays

GST pull-down assays were performed using the MicroSpin GST Purification Module (Amersham Biosciences) according to the manufacturer's protocol. GST constructs were transformed into BL21-Gold (DE3) cells (Stratagene) for protein induction. Transformed cells were grown at 37°C to OD_{A600}=0.8 and GST proteins were induced for 1.5 hours at 20–27°C with 1 mM IPTG (Amersham Biosciences). Hemagglutinin (HA)-tagged putative interacting proteins were produced in 293T cells. Lysates were sonicated three times for 10 seconds prior to centrifugation at 16,000 ***g*** at 4°C for 10 minutes, and the supernatant was collected. GST-fusion protein lysates and putative interacting protein lysates were loaded on GST columns,

incubated for 1.5 hours at 25°C, eluted, electrophoresed on a 12% SDS-PAGE gel and transferred to PolyScreen PVDF Transfer Membranes. HA-tagged proteins were detected with mouse HA.11 primary antibody (1:1,000, Covance Research Products) and with peroxidase-conjugated AffiniPure donkey anti-mouse (H+L) secondary antibody (1:10,000, Jackson ImmunoResearch Laboratories). GST-fusion proteins were detected with rabbit anti-GST primary antibody (1:25,000, Sigma-Aldrich) and with peroxidase-conjugated AffiniPure donkey anti-rabbit (H+L) secondary antibody (1:10,000, Jackson ImmunoResearch Laboratories).

Results

TBX5 and TBX20 are required for heart morphogenesis

To analyze the requirement for *Tbx5* and *Tbx20* in cardiogenesis, antisense morpholinos were designed against the 5′UTRs and translational start sites of the respective cDNAs (Fig. 1A) (Heasman et al., 2000). Owing to the lack of antibodies against endogenous TBX5 or TBX20, we tested the efficiency and specificity of morpholino translation inhibition using V5 epitope-tagged versions of TBX5 and TBX20 both in vitro and in vivo. To this end, transcription/translation reactions were incubated with each cDNA construct alone and together with increasing concentrations of morpholinos (Fig. 1B,C). TBX20MO was included as control for TBX5MO and vice versa, and a ControlMO used for both. Results from these assays show that TBX5MO blocks translation of TBX5-V5 while TBX20MO and ControlMO do not. Similarly, TBX20MO blocks translation of TBX20-V5 in vitro (Fig. 1B,C).

To determine if TBX5MO and TBX20MO block translation in vivo, we injected *Tbx5-V5* or *Tbx20-V5* mRNA alone or in the presence of morpholinos into one-cell stage embryos. Animal caps were cut at stage 8 and allowed to develop to stage 10, at which point western blot analyses were performed. Results from these studies demonstrate that in animal caps, TBX5MO blocks TBX5-V5 translation, while TBX20MO blocks TBX20-V5 translation (Fig. 1D,E). We have further shown via sequence alignments that *Tbx5* does not contain binding sites for the *Tbx20* morpholinos and vice versa (see Fig. S1 in the supplementary material). We did note that the introduction of TBX20MO results in a slight decrease in TBX5 in vivo, and vice versa (see Discussion).

To determine the requirement of TBX5 and TBX20 in heart development, we injected TBX5MO, TBX20MO, or ControlMO into one-cell stage embryos. No significant differences are seen between TBX5 morphants, TBX20 morphants, control morphants, or uninjected siblings throughout gastrulation and neurulation stages. However, a slight delay in developmental stage is evident in TBX5 and TBX20 morphants relative to control morphants and uninjected embryos by neurulation stages (~stage 16). By cardiac looping stages (~stage 38) (Kolker et al., 2000; Mohun and Leong, 1999; Mohun, 2000; Newman and Krieg, 1999), a reduction in cardiac mass is evident in the morphants, and by stage 38 both morphants display grossly abnormal heart morphology (Fig. 2A–F). At this stage, 82% of TBX5 morphants and 100% of TBX20 morphants display prominent cardiac defects, as scored by the presence of an unlooped heart tube, a reduction in cardiac mass and the presence of a pericardial edema (Fig. 2G). After terminal cardiomyocyte differentiation has begun (~stage 45) (Kolker et al., 2000; Mohun and Leong, 1999; Mohun et al., 2000; Newman and Krieg, 1999), TBX5 and TBX20 morphants display dramatically smaller hearts and in many embryos cardiac tissue is barely detectable (Fig. 2E,F). However, the remaining cardiac tissue still retains some degree of contractility, although it is confined to a small patch of contractile tissue in the dorsal-most aspect of the cardiac cavity. Both TBX5 and TBX20 morphants also display abnormal eyes, which is consistent with studies showing the involvement of both genes in eye development (Fig. 2) (Carson et al., 2004; Koshiba-Takeuchi et al., 2000; Leconte et al., 2004). Embryos derived from injection of *Tbx20* morpholinos directed against the antisense transcript, *Tbx5*

morpholinos containing mismatches, MOs directed against zebrafish *Tbx5* and Gene Tools LLC's MO control, produced no observable phenotype at any concentration (data not shown). These observations, and the findings that the TBX5 and TBX20 protein levels can be reduced or eliminated both in vitro and in vivo, suggest that the phenotypes we observe are specific for knocking down TBX5 and TBX20.

To further define the requirements for *Tbx5* and *Tbx20* during cardiogenesis, we carried out a detailed analysis of TBX5MO-and TBX20MO-derived hearts relative to those from ControlMO injections. For these analyses, staged-matched TBX5MO, TBX20MO and ControlMO embryos were collected at stage 37, serial sectioned and stained for the terminal differentiation markers tropomyosin and cardiac actin, and counterstained with DAPI (Fig. 3). Results from this analysis clearly demonstrate that TBX5MO- and TBX20MO-derived hearts fail to undergo cardiac looping and chamber formation. In addition, quantification of total cardiac cell number by serial sectioning shows that both TBX5MO and TBX20MO hearts have a significant reduction in cell number compared with controls, and TBX20MO-derived hearts have significantly fewer cardiomyocytes than those from TBX5MO (Fig. 3M).

In addition to these defects, we note some features unique to both the TBX5MO- and TBX20MO-derived hearts, most notably TBX5MO hearts remain as an open cardiac trough (Mohun et al., 2000) throughout development and fail to form a cardiac tube (Fig. 3E–H). By contrast, TBX20MO-derived embryos form a cardiac tube; however, the lumen often collapses. We also note a decrease in cardiac actin in TBX20MO-derived hearts (Fig. 3L) compared with TBX5MO or control hearts (Fig. 3D,H). Together, these data demonstrate a requirement for both *Tbx5* and *Tbx20* in normal heart morphogenesis, and imply that TBX5 cannot compensate for the loss of TBX20 nor can TBX20 compensate for the loss of TBX5. They also suggest that *Tbx5* and *Tbx20* play non-redundant roles during normal heart development.

Analysis of hearts derived from TBX5MO and TBX20MO embryos shows a significant decrease in cardiac cell number. To determine if this is due to alterations in cardiac cell commitment, we performed whole-mount in situ hybridization with the early heart marker, *Nkx2.5* (Fig. 4). This analysis was carried out on staged-matched embryos derived from TBX5MO, TBX20MO and ControlMO embryos over the period of cardiac cell commitment, migration and differentiation (stages 16–36). We could not detect any obvious difference in the number or spatial distribution of *Nkx2.5*-expressing cells prior to stage 24 (Fig. 4). Consistent with our initial analysis, after stage 24, the hearts from TBX5MO and TBX20MO embryos are morphologically abnormal and smaller in size, and therefore show a reduced domain of *Nkx2.5* expression.

The above results demonstrate that *Tbx5* and *Tbx20* are required for normal heart morphogenesis, but not for specification and migration of the cardiac precursors. To extend these findings, in situ hybridization was performed on stage 36 morphants and controls using the late heart markers *atrial natriuretic factor* (*XANF*) (Small and Krieg, 2000) and *cardiac troponin I* (*XTnIc*) (Drysdale et al., 1994). As shown in Fig. 5, the terminally differentiated cardiomyocyte marker *XTnIc* displays properly localized expression in the cardiac tissue of morphant embryos and appears to be expressed to the same degree, although owing to the reduced cardiac mass, it is expressed in fewer cells (Fig. 5D–F). *XANF* is a putative target of *Tbx5*, and its expression is reduced in the absence of *Tbx5* in mice (Bruneau et al., 2001). In agreement with these findings, we show that *Xenopus* TBX5 activates transcription of a rat *Nppa/ANF* reporter plasmid (Fig. 6) and, consistent with TBX5MO blocking TBX5, *XANF* expression is either greatly reduced or absent in TBX5 morphants; however, *XANF* is still detected in TBX20 morphants (Fig. 5A–C). These results indicate that terminal differentiation still occurs in both TBX5 and TBX20 morphant embryos and implies that *XANF* is an evolutionarily conserved target of TBX5.

Tbx5 and *Tbx20* are not dependent on the expression of one another

As *Tbx5* and *Tbx20* are co-expressed within the heart and have similar requirements in heart development, we next asked whether *Tbx5* and *Tbx20* function linearly within the same molecular pathway. To address this question, we analyzed the expression of *Tbx20* in TBX5MO-injected embryos and *Tbx5* expression in TBX20MO-injected embryos. We could detect no differences in the expression of either gene in morpholino-injected embryos (Fig. 7); both genes remain expressed in the forming heart tissue, despite the reduction of cardiac tissue mass in morpholino-injected embryos. Based on these results, we conclude TBX5 is not essential for *Tbx20* expression, nor is *Tbx20* dependent on TBX5.

TBX20 affects TBX5 transcriptional activity

Our results strongly suggest that *Tbx5* and *Tbx20* do not function linearly within the same pathway, yet have a similar requirement in heart development. We therefore carried out a series of experiments to test if TBX5 and TBX20 have either competing or complimentary functions at the molecular level. We first tested the cellular localization of TBX5 and TBX20. For these studies, V5 epitope-tagged versions of the full-length cDNAs were transfected into NIH/3T3 cells. Immunohistochemistry on the transfected cells show that similar to TBX5 (Collavoli et al., 2003; Fan et al., 2003; Zaragoza et al., 2004), TBX20 is localized exclusively to the nucleus (Fig. 6C–H).

We next tested whether TBX5 and TBX20 can function to regulate the levels of transcription of the TBX5 target gene *Nppa/ANF*. To test for DNA-specific binding and transcriptional activities, we transfected in full-length versions of *Tbx5* and *Tbx20*, either alone or in combination, with the putative *Tbx5* target *Nppa/ANF* reporter construct into 293T cells. Consistent with studies using the mouse *Tbx5* ortholog (Bruneau et al., 2001; Hiroi et al., 2001), TBX5 can weakly activate the rat *Nppa/ANF* reporter. By contrast, *Tbx20* alone can activate *Nppa/ANF* in a dose dependent fashion. However, in the presence of TBX5, TBX20 can have the converse effect on the *Nppa/ANF* reporter. In the presence of TBX5, at high and low doses of TBX20 there is increased activation of the reporter construct, while at moderate doses there is a repressive effect (Fig. 6I). Thus, the presence of TBX5 appears to alter TBX20 transcriptional activity.

TBX5 and TBX20 physically interact with one another

Given the similarity in phenotypes of TBX5 and TBX20 morphant embryos, and the observation that *Tbx5* and *Tbx20* are not dependent on the expression of one another, we next assessed whether TBX5 and TBX20 can physically interact. TBX5 fused to Glutathione-S-Transferase (GST) was incubated with HA-tagged TBX20 or NKX2-5. Pull-down experiments were then performed to assess whether TBX20 can bind to TBX5. NKX2-5 has been shown to interact with TBX5 and thus serves as a positive control (Bruneau et al., 2001; Hiroi et al., 2001). As shown in Fig. 8A, bacterially translated GST-TBX5 is able to bind HA-TBX20 and HA-NKX2-5 produced from 293T cells, in contrast to GST alone, which does not bind either protein. These results reveal that TBX5 and TBX20 can interact in vitro. This is the first report of physical interaction between T-box proteins.

Having demonstrated that TBX5 and TBX20 interact, we next mapped the interaction domains of TBX5 and TBX20. To this end, we constructed a deletion series of both GST-tagged TBX5 and HA-tagged TBX20. As shown in Fig. 8C, GST-TBX5 proteins lacking the C terminus still bind HA-TBX20; however, when the small N terminus and T-box domain are removed from GST-TBX5, HA-TBX20 fails to bind. Thus, the domain responsible for TBX20 binding lies within the N-terminus and T-domain of TBX5. Similarly, a C-terminal deletion of HA-TBX20 still binds to GST-TBX5, in contrast to deletions of the HA-TBX20 N-terminus and T-domain (Fig. 8E). As seen in the ΔN/C lane in Fig. 8E, the HA-TBX20 deletion containing only the

T-box domain did not bind GST-TBX5. However, we were unable to obtain comparable amounts of the HA-T20-ΔN/C protein, as seen in the input lane. This could be due to mRNA or protein instability. In an attempt to circumvent this problem, the amount of HA-T20-ΔN/C protein incubated with GST-TBX5 was increased twofold compared with the rest of the experiments. These results indicate that the N terminus and possibly the T-domain of TBX20 are required for its interaction with TBX5, although we cannot rule out the possibility that the amount of HA-T20-ΔN/C protein was insufficient to identify a requirement for the T-domain. In summary, our results reveal that the domains responsible for the interaction between TBX20 and TBX5 map to within the N-terminal and T-box domains in both proteins.

Tbx5 and *Tbx20* cooperate to regulate heart morphogenesis

Given that TBX5 and TBX20 physically interact with one another, we hypothesized that *Tbx5* and *Tbx20* may function cooperatively to control cardiogenesis. To test this hypothesis, we co-injected concentrations of TBX5MO and TBX20MO below the threshold at which cardiac phenotypes are efficiently induced when injected individually. At a concentration of 40 ng per embryo for *Tbx5* morpholinos and 80 ng per embryo for *Tbx20* morpholinos, injections yield consistent heart phenotypes in 82% of TBX5MO-injected embryos and in 100% of TBX20MO-injected embryos (Fig. 2). We refer to this dose as the ‘optimal’ dose, because it is the dose that efficiently blocks translation of Tbx5 and Tbx20 in vivo (Fig. 1D,E) and the dose that gives efficient and penetrant cardiac phenotypes. At half doses, 20 ng per embryo for TBX5MO and 40 ng per embryo for TBX20MO, each morpholino yields significantly fewer and weaker heart phenotypes compared with the full dose (Fig. 9M, data not shown). We refer to this concentration as the ‘suboptimal’ dose for inducing cardiac defects. The terms ‘optimal’ and ‘suboptimal’ are only used to refer to the concentrations that yield fully penetrant or partially penetrant cardiac phenotypes, respectively.

To address the question of whether *Tbx5* and *Tbx20* cooperate in cardiogenesis, we injected TBX5MO and TBX20MO individually at suboptimal doses in combination with ControlMO to keep total morpholino concentrations equal in all injections. TBX5MO was then co-injected with TBX20MO, each at the suboptimal dose. ControlMO injected at 80 ng/embryo served as control. As shown in Fig. 9, only 4% of embryos injected with suboptimal TBX5MO/ControlMO displayed a pericardial edema, unlooped heart tubes and a reduction in cardiac mass. Suboptimal TBX20MO/ControlMO yields only 13% cardiac defects. In suboptimal injections, the majority of embryos appeared normal, while the few cardiac phenotypes produced were much less severe than at optimal doses (e.g. barely detectable reduction in cardiac mass, slight perturbation of looping and little or no pericardial edema). When co-injected at suboptimal doses, 74% of TBX5MO/TBX20MO co-injected embryos display dramatic cardiac defects compared with 0% of ControlMO-injected embryos (Fig. 9A–L). The observation that the percentage of heart defects in double morphants is more than additive suggests that *Tbx5* and *Tbx20* synergistically act to control heart morphogenesis.

If *Tbx5* and *Tbx20* cooperate to regulate cardiogenesis, one might expect a more severe alteration in cardiac morphology and marker expression when the levels of both proteins are reduced. To address this issue, we performed in situ hybridization on stage 36 embryos from the above double injection experiment using *Nkx2-5*, *XANF* and *XTnIc* probes. As shown in Fig. 9, all three markers are expressed normally in embryos injected with suboptimal doses of TBX5MO and TBX20MO when compared with ControlMO. However, heart marker expression in the double morphant embryos is markedly reduced, particularly *XANF*. Both *Nkx2-5* and *XTnIc* are still detectable in the heart region, albeit in fewer cells. Thus, the synergistic cooperation of TBX5 and TBX20 are required for proper heart development.

Discussion

Members of the T-box family of proteins play a fundamental role in patterning the developing vertebrate heart; however, the precise cellular requirements for any one family member remains largely unknown. In this study, we demonstrate that TBX5 and TBX20 are both required for early cardiac morphogenesis. Moreover, we show that TBX5 and TBX20 function in the same pathway, implying a synergistic role for these two proteins during early heart development. Consistent with this proposal, we show that TBX5 and TBX20 can physically and functionally interact, therefore providing the first evidence for direct interaction between members of the T-box gene family.

Functions of *Tbx5* and *Tbx20* in cardiac morphogenesis

Our studies show that *Tbx5* and *Tbx20* are required for similar cellular processes in the developing heart. These data demonstrate a non-redundant function for TBX5 and TBX20 during cardiac morphogenesis; neither protein can compensate for the other in heart morphogenesis. The lack of redundancy at the molecular level is corroborated by the observation that the putative TBX5 target gene *XANF* either is not expressed or is expressed very weakly in TBX5 morphant embryos, while being expressed at the proper time, place and levels in TBX20 morphant embryos. Together, these data suggest that TBX5 and TBX20 act in a non-redundant fashion to control morphogenetic movements of early heart tissue.

The cardiac defects, in response to a reduction of either TBX5 or TBX20, appear to represent a block in an early morphological step in heart formation. As the spatial distribution of *Nkx2-5* is unaltered throughout early development in TBX5MO-, TBX20MO- and ControlMO-injected embryos, and as *Nkx2.5*, *Tbx5* and *Tbx20* continue to be expressed until the later stages of heart development, and TBX5 and TBX20 morphants express markers of terminal muscle differentiation, neither *Tbx5* nor *Tbx20* appears to be required for commitment, migration or terminal differentiation of cardiac tissue. Thus, both *Tbx5* and *Tbx20* appear to be required to direct the coordinated events that occur during the early steps of heart morphogenesis.

Consistent with this hypothesis, both TBX5 and TBX20 morphant-derived hearts are greatly extended along the anteroposterior axis, and the heart tube fails to correctly loop and undergo chamber formation. As a result, embryos display pericardial edemas, have impaired blood flow (see Figs S2 and S3 in the supplementary material), an irregular heartbeat (data not shown) and ultimately die. Thus, the alteration in heart morphology appears to be the primary outcome of perturbing TBX5 or TBX20 function.

Past attempts to interfere with *Tbx5* function in *X. laevis* were carried out by the misexpression of a putative interfering form of *Tbx5* that leads to either the absence or severe malformations of the heart (Horb and Thomsen, 1999). In instances in which the heart does form, there is a reduction or block in myocardial tissue formation and a failure of the heart to undergo looping. Our results with *Tbx5*-specific morpholinos show a less severe heart phenotype than those reported with the dominant interfering *Tbx5* but bear a close resemblance to those reported for the zebrafish *Tbx5* mutant, *heartstrings* (Garrity et al., 2002). This may be due to the dominant-interfering form of *Tbx5* used in the *X. laevis* studies interfering with the function of both *Tbx5* and *Tbx20* or possibly other T-box family members expressed in the developing heart, e.g. *Tbx1* and *Tbx2* (Chapman et al., 1996), as has been shown for other *Engrailed* fusions (Horb and Thomsen, 1997). However, in the absence of a TBX5-specific antibody, we cannot rule out the possibility that some residual TBX5 protein is present in morphant embryos leading to a less severe phenotype in our studies.

Tbx5 and Tbx20 are not dependent on the function of one another

The phenotypes of TBX5 and TBX20 morphant embryos do not appear to act in a linear pathway as the spatial and temporal expression of *Tbx5* appears unaltered in TBX20 morphants, and vice versa. These findings are in agreement with studies showing normal expression of *Tbx20* in *Tbx5* mutant mice (Bruneau et al., 2001) but in apparent conflict with a second study reporting the downregulation of *Tbx5* in zebrafish embryos injected with a *Tbx20* morpholino (Szeto et al., 2002). Although the zebrafish and *X. laevis* orthologs of *Tbx20* share a very high degree of identity at the protein level (86%), the differences between the two orthologs may reflect a species difference as, for example, has been reported for the endodermal-inducing activities of the T-box-containing gene *Brachyury* (Marcellini et al., 2003). Although no alterations in *Tbx5* or *Tbx20* RNA levels were observed in morphant embryos, we did observe a downregulation of TBX5 protein in response to *Tbx20* morpholinos in vivo, and vice versa, but not in vitro (Fig. 1), raising the interesting possibility that cross-regulation may be occurring between TBX5 and TBX20 at the level of translation. As similar studies have not been conducted in zebrafish, it is not possible at this time to know the mechanisms of crossregulation or whether this is a conserved response to interfering with TBX5 or TBX20.

TBX5 and TBX20 heterodimerization

Although *Tbx5* and *Tbx20* are co-expressed and both function in early heart development, the genes appear to be regulated through separate pathways. For example, *Tbx20* but not *Tbx5* can be induced in response to *BMP2* signaling (Plageman and Yutzey, 2004). Taken together with our results demonstrating a physical interaction between TBX5 and TBX20, these data would suggest that TBX5 and TBX20 function in parallel pathways that converge upon TBX5:TBX20 heterodimerization. This model is also supported by our results showing a functional interaction between TBX5 and TBX20: embryos derived from injections of suboptimal doses of *Tbx5* and *Tbx20* morpholinos have only minor effects on heart development in a small proportion of the embryos. However, when injected in combination, 74% of all embryos examined displayed grossly abnormal heart formation.

What are the possible cellular functions of TBX5 and TBX20 in heart development? Past studies of T-box genes have shown a direct link between members of the T-box gene family and cell adhesion. For example, embryos homozygous for mutations in *Brachyury*, the founding member of the T-box gene family, show an inability of the mesoderm to migrate properly along the extracellular matrix leading to an inability of the mesodermal germ layer to complete the morphogenetic movements normally associated with gastrulation (reviewed by Showell et al., 2004). We propose an analogous model for TBX5 and TBX20 function in regulating cell polarity or adhesion events associated with heart morphogenesis. We propose that TBX5 and TBX20 function to control polarity or adhesive properties of cardiac tissue once the two heart fields merge along the anterior midline, and that target specificity is regulated through TBX5 and TBX20 protein-protein interactions. In agreement with this proposal, we have recently shown that alterations in cardiac cell numbers, survival and proliferation in TBX5MO-derived embryos are a secondary consequence of disrupting TBX5 function (S. Goetz and F.L.C., unpublished). This observation, taken together with our findings that cardiac gene expression patterns are not disrupted in TBX5MO- or TBX20MO-derived embryos, suggests that the primary role for TBX5 and TBX20 is to control cardiac cell polarity or adhesion.

It is worth noting that neither TBX5 nor TBX20 have strong transcriptional activation or repression activity by themselves (Fig. 6) (Bruneau et al., 2001;Hiroi et al., 2001;Plageman and Yutzey, 2004;Stennard et al., 2003). Thus, transcriptional activity appears to be governed by protein-protein interactions. Past studies have identified several other interacting partners for both TBX5 and TBX20. For example, both TBX5 and TBX20 have been shown to interact

with the homeobox-containing transcription factor NKX2-5 (Bruneau et al., 2001;Hiroi et al., 2001;Stennard et al., 2003), consistent with clinical studies showing that HOS patients and humans heterozygous for NKX2-5 display many of the same cardiac defects (Elliott et al., 2003;Goldmuntz et al., 2001;Prall et al., 2002).

How might TBX5:TBX20 heterodimerization affect target choice? It is possible that the role of TBX5:TBX20 dimerization is to sequester TBX5 and thereby block its interaction with other proteins such as NKX2.5, thereby indirectly inhibiting the induction of cardiac specific genes such as *XANF*. However, several lines of evidence argue against such a proposal. For example, at low and high concentrations TBX20 can increase transcription of the *Nppa/ANF* reporter in the presence of TBX5, while showing a repressive activity at intermediate concentrations, suggesting that in certain contexts TBX20 can cooperate with TBX5 to activate transcription, while antagonizing TBX5 activity in others. An alternative possibility is that TBX20 target choice and ability to function as a transcriptional activator or repressor is governed by its choice of interacting partners. Consistent with this hypothesis, Stennard et al. (Stennard et al., 2003) have shown that NKX2.5, GATA4 and GATA5 interact with TBX20, and the interactions occur through the same domain of TBX20 that we have shown interacts with TBX5, at least in the cases of NKX2.5 and GATA4. Furthermore, the authors have demonstrated that TBX20 can repress synergistic activation of a connexin 40 reporter by NKX2.5 and GATA4, while synergistically activating the same reporter with NKX2.5 and GATA5. Thus, TBX20 may be able to function both as a transcriptional activator or repressor, and this decision is based on its choice of protein partners. In addition, TBX5 and TBX20 have been shown to display different binding affinities for different T-box-binding sites (Stennard et al., 2003). For example, TBX20, unlike TBX5 can bind to the *Brachyury* target site while TBX5 has a higher affinity than TBX20 for the T-box binding site in the *Nppa*/*ANF* promoter. Thus, downstream target selection may be dictated by homodimerization versus heterodimerization. This is supported by the recent findings that several genes involved in heart development are found to contain multiple T-box binding sites (R. Schwartz, personal communication; F.L.C., unpublished). Our model suggests that TBX5 and TBX20 target selection and transcriptional activity is based on partner choice in a specific tissue at a specific time. However, it still remains to be established which protein interactions take place in the developing heart and in turn, what governs the choice of partners for TBX5 or TBX20. These are presently areas under active investigation.

Acknowledgements

This work is supported by grants from the NIH and AHA, and by an award from the UNC Medical Alumni Association. D.D.B. is funded by a NSF fellowship. The tropomyosin antibody developed by J.-C. Lin was obtained from the Developmental Studies Hybridoma Bank developed under the auspices of the NICHD and maintained by the University of Iowa, Department of Biological Sciences, Iowa City, IA 52242. We thank Bahay Gulle for help generating constructs, Judy Chang, Amanda Marshburn, Kristian Duggan, Caroline Collins, Hui-Hua Li and Cam Patterson for assistance. We also thank Chris Showell and Larysa Pevny for critical reading of the manuscript and helpful suggestions.

References

Baldini A. DiGeorge syndrome: an update. Curr Opin Cardiol 2004;19:201–204. [PubMed: 15096950]

Basson CT, Bachinsky DR, Lin RC, Levi T, Elkins JA, Soults J, Grayzel D, Kroumpouzou E, Traill TA, Leblanc Straceski J, et al. Mutations in human cause limb and cardiac malformation in Holt-Oram syndrome. Nat Genet 1997;15:30–35. [PubMed: 8988165]

Basson CT, Huang T, Lin RC, Bachinsky DR, Weremowicz S, Vaglio A, Bruzzone R, Quadrelli R, Lerone M, Romeo G, et al. Different TBX5 interactions in heart and limb defined by Holt-Oram syndrome mutations. Proc Natl Acad Sci USA 1999;96:2919–2924. [PubMed: 10077612]

Benson DW, Basson CT, MacRae CA. New understandings in the genetics of congenital heart disease. Curr Opin Pediatr 1996;8:505–511. [PubMed: 8946132]

Brown DD, Binder O, Pagratis M, Parr BA, Conlon FL. Developmental expression of the Xenopus laevis Tbx20 orthologue. Dev Genes Evol 2003;212:604–607. [PubMed: 12536325]

Bruneau BG, Nemer G, Schmitt JP, Charron F, Robitaille L, Caron S, Conner DA, Gessler M, Nemer M, Seidman CE, et al. A murine model of Holt-Oram syndrome defines roles of the T-Box transcription factor Tbx5 in cardiogenesis and disease. Cell 2001;106:709–721. [PubMed: 11572777]

Carson CT, Pagratis M, Parr BA. Tbx12 regulates eye development in Xenopus embryos. Biochem Biophys Res Commun 2004;318:485–489. [PubMed: 15120626]

Chapman DL, Garvey N, Hancock S, Alexiou M, Agulnik SI, Gibson-Brown J, Cebra-Thomas J, Bollag R, Silver LM, Papaionnou VE. Expression of the T-box family genes, *Tbx1-Tbx5*, during early mouse development. Dev Dyn 1996;206:379–390. [PubMed: 8853987]

Chieffo C, Garvey N, Gong W, Roe B, Zhang G, Silver L, Emanuel BS, Budarf ML. Isolation and characterization of a gene from the DiGeorge chromosomal region homologous to the mouse Tbx1 gene. Genomics 1997;43:267–277. [PubMed: 9268629]

Collavoli A, Hatcher CJ, He J, Okin D, Deo R, Basson CT. TBX5 nuclear localization is mediated by dual cooperative intramolecular signals. J Mol Cell Cardiol 2003;35:1191–1195. [PubMed: 14519429]

Cripps RM, Olson EN. Control of cardiac development by an evolutionarily conserved transcriptional network. Dev Biol 2002;246:14–28. [PubMed: 12027431]

Drysdale TA, Tonissen KF, Patterson KD, Crawford MJ, Kreig PA. Cardiac troponin I is a heart specific marker in the Xenopus embryo: expression during abnormal heart heart morphogenesis. Dev Biol 1994;154:432–441. [PubMed: 7958411]

Elliott DA, Kirk EP, Yeoh T, Chandar S, McKenzie F, Taylor P, Grossfeld P, Fatkin D, Jones O, Hayes P, et al. Cardiac homeobox gene NKX2-5 mutations and congenital heart disease: associations with atrial septal defect and hypoplastic left heart syndrome. J Am Coll Cardiol 2003;41:2072–2076. [PubMed: 12798584]

Fan C, Liu M, Wang Q. Functional analysis of TBX5 missense mutations associated with Holt-Oram syndrome. J Biol Chem 2003;278:8780–8785. [PubMed: 12499378]

Garrity DM, Childs S, Fishman MC. The heartstrings mutation in zebrafish causes heart/fin Tbx5 deficiency syndrome. Development 2002;129:4635–4645. [PubMed: 12223419]

Goldmuntz E, Geiger E, Benson DW. NKX2.5 mutations in patients with tetralogy of fallot. Circulation 2001;104:2565–2568. [PubMed: 11714651]

Harland RM. In situ hybridization: an improved whole mount method for Xenopus embryos. Methods Cell Biol 1991;36:675–685. [PubMed: 1811159]

Harvey RP. Patterning the vertebrate heart. Nat Rev Genet 2002;3:544–556. [PubMed: 12094232]

Heasman J, Kofron M, Wylie C. Beta-catenin signaling activity dissected in the early Xenopus embryo: a novel antisense approach. Dev Biol 2000;222:124–134. [PubMed: 10885751]

Hiroi Y, Kudoh S, Monzen K, Ikeda Y, Yazaki Y, Nagai R, Komuro I. Tbx5 associates with Nkx2-5 and synergisticallly promotes cardiomyocyte differentiation. Nat Genet 2001;28:276–280. [PubMed: 11431700]

Hoffman JI. Incidence of congenital heart disease: I. Postnantal incidence. Pediatr Cardiol 1995a;16:103–113. [PubMed: 7617503]

Hoffman JI. Incidence of congenital heart disease: II Prenatal incidence. Pediatr Cardiol 1995b;16:155–165. [PubMed: 7567659]

Horb ME, Thomsen GH. A vegetally localized T-box transcription factor in Xenopus eggs specifies mesoderm and endoderm and is essential for embryonic mesoderm formation. Development 1997;124:1689–1698. [PubMed: 9165117]

Horb ME, Thomsen GH. Tbx5 is essential for heart development. Development 1999;126:1739–1751. [PubMed: 10079235]

Jerome LA, Papaioannou VE. DiGeorge syndrome phenotype in mice mutant for the T-box gene, Tbx1. Nat Genet 2001;27:286–291. [PubMed: 11242110]

Kolker S, Tajchman U, Weeks DL. Confocal Imaging of early heat development in Xenopus laevis. Dev Biol 2000;218:64–73. [PubMed: 10644411]

Koshiba-Takeuchi K, Takeuchi JK, Matsumoto K, Momose T, Uno K, Hoepker V, Ogura K, Takahashi N, Nakamura H, Yasuda K, et al. Tbx5 and the retinotectum projection. Science 2000;287:134–137. [PubMed: 10615048]

Laverriere AC, MacNeill C, Mueller C, Poelmann RE, Burch JB, Evans T. GATA-4/5/6, a subfamily of three transcription factors transcribed in developing heart and gut. J Biol Chem 1994;269:23177–23184. [PubMed: 8083222]

Leconte L, Lecoin L, Martin P, Saule S. Pax6 interacts with cVax and Tbx5 to establish the dorsoventral boundary of the developing eye. J Biol Chem 2004;279:47272–47277. [PubMed: 15322073]

Li QY, Newbury Ecob RA, Terrett JA, Wilson DI, Curtis AR, Yi CH, Gebuhr T, Bullen PJ, Robson SC, Strachan T, et al. Holt-Oram syndrome is caused by mutations in TBX5, a member of the Brachyury (T) gene family. Nat Genet 1997;15:21–29. [PubMed: 8988164]

Lindsey EA, Vitelli F, Su H, Morishima M, Huynh T, Pramparo T, Jurecic V, Ogunrinu G, Sutherland HF, Scrambler PJ, et al. Tbx1 haploinsufficiency in the DiGeorge syndrome region causes aortic arch defects in mice. Nature 2001;410:97–101. [PubMed: 11242049]

Logan M, Mohun T. Induction of cardiac muscle differentiation in isolated animal pole explants of Xenopus laevis embryos. Development 1993;118:865–875. [PubMed: 8076523]

Marcellini S, Technau U, Smith JC, Lemaire P. Evolution of Brachyury proteins: identification of a novel regulatory domain conserved within Bilateria. Dev Biol 2003;260:352–361. [PubMed: 12921737]

Merscher S, Funke B, Epstein JA, Heyer J, Puech A, Lu MM, Xavier RJ, Demay MB, Russell RG, Factor S, et al. TBX1 is responsible for cardiovascular defects in velo-cardio-facial/DiGeorge syndrome. Cell 2001;104:619–629. [PubMed: 11239417]

Mohun, T. J. and Leong, L. M. (1999). *Heart Formation and the Heart Field in Amphibian Embryos* San Diego, CA: Academic Press.

Mohun TJ, Leong LM, Weninger WJ, Sparrow DB. The morphology of heart development in Xenopus laevis. Dev Biol 2000;218:74–88. [PubMed: 10644412]

Moskowitz IP, Pizard A, Patel VV, Bruneau BG, Kim JB, Kupershmidt S, Roden D, Berul CI, Seidman CE, Seidman JG. The T-Box transcription factor Tbx5 is required for the patterning and maturation of the murine cardiac conduction system. Development 2004;131:4107–4116. [PubMed: 15289437]

Newbury-Ecob R, Leanage R, Raeburn JA, Young ID. The Holt-Oram Syndrome: a clinical genetic study. J Med Genet 1996;33:300–307. [PubMed: 8730285]

Newman, C. S. and Krieg, P. A. (1999). *Specification and Differentiation of the Heart in Amphibia* San Diego, CA: Academic Press.

Nieuwkoop, P. D. and Faber, J. (1967). *Normal Table of* Xenopus laevis *(Daudin)* Amsterdam, The Netherlands: North Holland.

Packham EA, Brook JD. T-box genes in human disorders. Hum Mol Genet 2003;12:R37–R44. [PubMed: 12668595]

Payne RM, Johnson MC, Grant JW, Strauss JE. Toward a molecular understanding of congenital heart disease. Circulation 1995;91:494–504. [PubMed: 7805255]

Plageman TF Jr, Yutzey KE. Differential expression and function of tbx5 and tbx20 in cardiac development. J Biol Chem 2004;279:19026–19034. [PubMed: 14978031]

Prall OW, Elliott DA, Harvey RP. Developmental paradigms in heart disease: insights from tinman. Ann Med 2002;34:148–156. [PubMed: 12173684]

Ryan K, Chin AJ. T-box genes and cardiac development. Birth Defects Res Part C Embryo Today 2003;69:25–37.

Serbedzija GN, Chen JN, Fishman MC. Regulation in the heart field of zebrafish. Development 1998;125:1095–1101. [PubMed: 9463356]

Showell C, Binder O, Conlon F. T-box genes in early embryogenesis. Dev Dyn 2004;229:201–218. [PubMed: 14699590]

Small EM, Krieg PA. Expression of atrial natriuretic factor (ANF) during Xenopus cardiac development. Dev Genes Evol 2000;210:638–640. [PubMed: 11151301]

Stennard FA, Costa MW, Elliott DA, Rankin S, Haast SJ, Lai D, McDonald LP, Niederreither K, Dolle P, Bruneau BG, et al. Cardiac T-box factor Tbx20 directly interacts with Nkx2-5, GATA4, and

GATA5 in regulation of gene expression in the developing heart. Dev Biol 2003;262:206–224. [PubMed: 14550786]

Szeto DP, Griffin KJ, Kimelman D. HrT is required for cardiovascular development in zebrafish. Development 2002;129:5093–5101. [PubMed: 12397116]

Tonissen KF, Drysdale TA, Lints TJ, Harvey RP, Krieg PA. XNkx-2.5, a Xenopus gene related to Nkx-2.5 and tinman: evidence for a conserved role in cardiac development. Dev Biol 1994;162:325–328. [PubMed: 7545912]

Wilson PA, Hemmati-Brivanlou A. Induction of epidermis and inhibition of neural fate by Bmp-4. Nature 1995;376:331–333. [PubMed: 7630398]

Yagi H, Furutani Y, Hamada H, Sasaki T, Asakawa S, Minoshima S, Ichida F, Joo K, Kimura M, Imamura S, et al. Role of TBX1 in human del22q11.2 syndrome. Lancet 2003;362:1366–1373. [PubMed: 14585638]

Zaffran S, Frasch M. Early signals in cardiac development. Circ Res 2002;91:457–469. [PubMed: 12242263]

Zaragoza MV, Lewis LE, Sun G, Wang E, Li L, Said-Salman I, Feucht L, Huang T. Identification of the TBX5 transactivating domain and the nuclear localization signal. Gene 2004;330:9–18. [PubMed: 15087119]

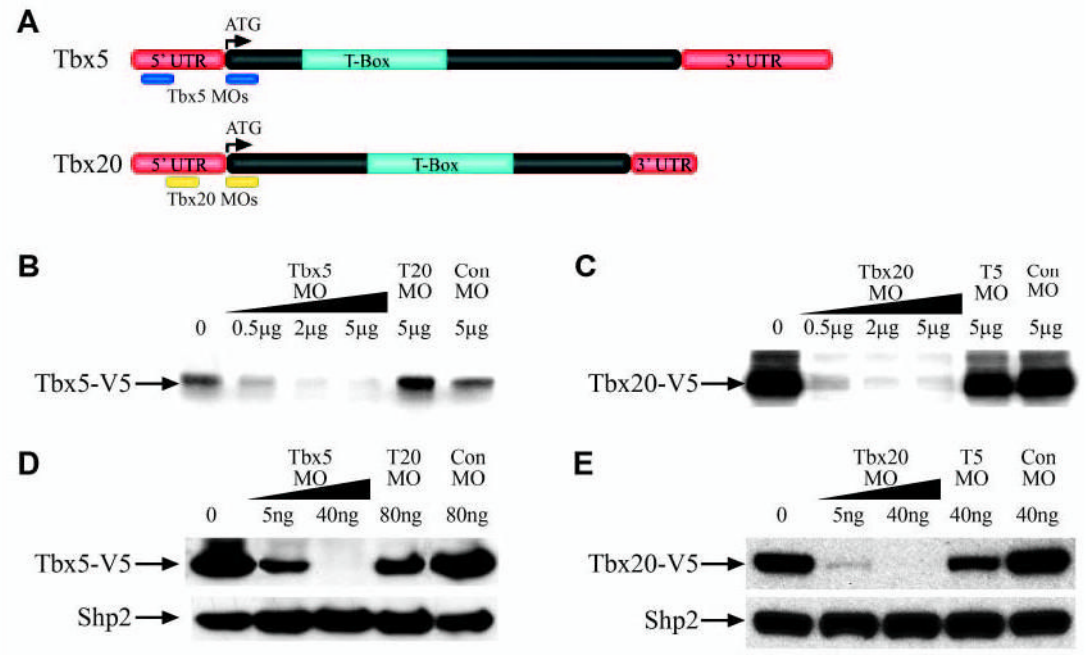

Fig. 1.

Tbx5 and *Tbx20* morpholinos block translation of their respective target proteins. (A) TBX5MO and TBX20MO positions relative to *Tbx5* and *Tbx20* cDNA. (B) Inhibition of TBX5-V5 translation in vitro by TBX5MO. TBX20MO and ControlMO serve as controls. Each reaction contains 1 μg of *Tbx5*-V5 circular plasmid along with the indicated amounts of MO. (C) Inhibition of TBX20-V5 translation in vitro by TBX20MO. TBX5MO and ControlMO serve as controls. Each reaction contains 1 μg of *Tbx20*-V5 circular plasmid along with the indicated amounts of MO. (D) Inhibition of TBX5-V5 translation by TBX5MO in animal caps. TBX20MO and ControlMO serve as controls. Probed with anti-V5 and re-probed with anti-PTP1D/SHP2 as a loading control. Embryos injected with 2 ng mRNA and the indicated amounts of MO. (E) Inhibition of TBX20-V5 translation by TBX20MO in animal caps. TBX20MO and ControlMO serve as controls. Probed with anti-V5 and re-probed with anti-PTP1D/SHP2 as a loading control. Embryos injected with 2 ng mRNA and the indicated amounts of MO.

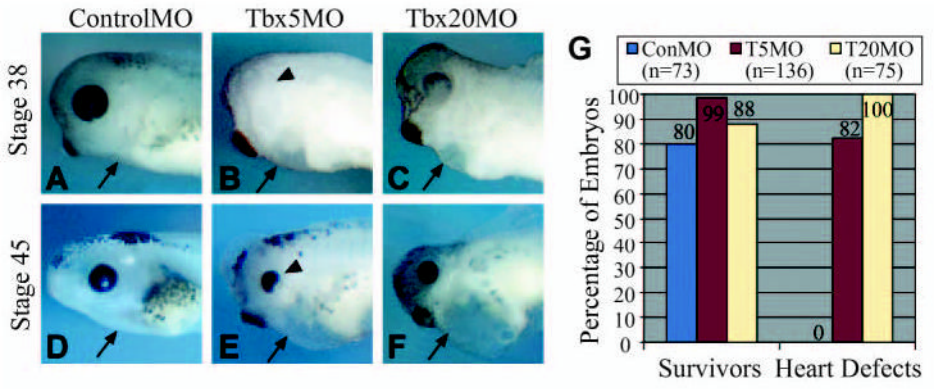

Fig. 2.

Tbx5 and *Tbx20* are required for proper cardiogenesis. (A–F) Morpholino-injected tadpoles at the indicated stages. Control morphant embryos (A,D), TBX5 morphant embryos (B,E) and TBX20 morphant embryos (C,F). Arrows indicate the heart region, arrowheads indicate the eye. (G) Chart displaying the percentage of morphants surviving and displaying cardiac abnormalities, as scored by the presence of an unlooped heart tube, a reduction in cardiac mass and the presence of a pericardial edema.

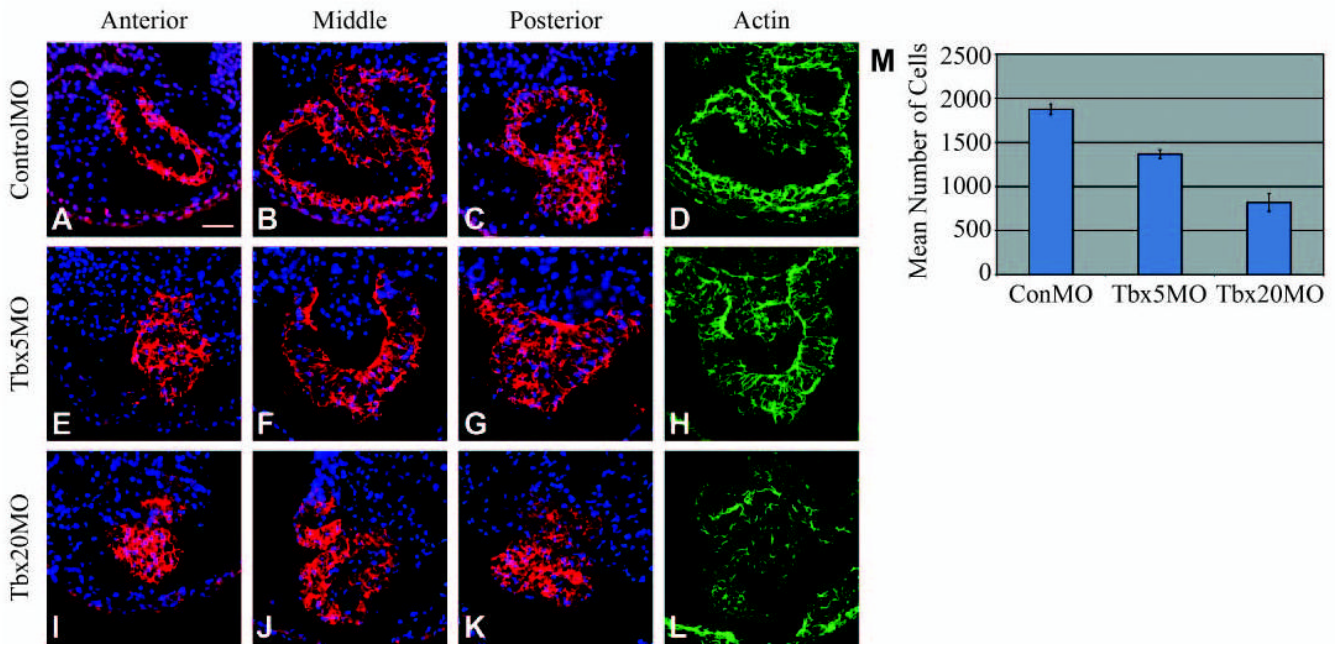

Fig. 3.

TBX5 and TBX20 morphants fail to undergo looping and chamber formation and display reduced cardiac cell numbers. Cryosections of TBX5 and TBX20 morphant hearts taken at the anterior (outflow), middle (ventricular) and posterior (atrial) regions. (A–D) ControlMO, (E–H) TBX5MO and (I–L) TBX20MO. Sections stained for tropomyosin (red), DAPI (blue) and cardiac actin (green). (D,H,L) Same sections as B, F and J stained with cardiac actin. In the looped control heart, the middle ventricular section also contains the atrium. (M) Mean number of cells per heart obtained by cell counts of heart tissue in serial sections derived from a minimum of three embryos.

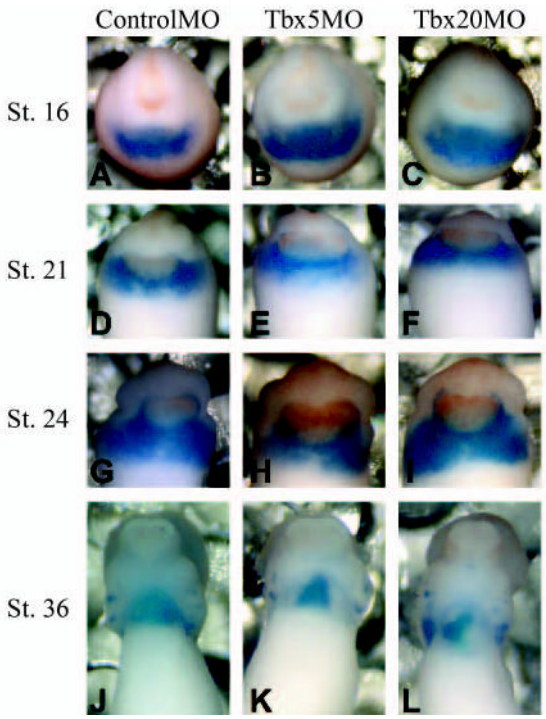

Fig. 4.

Cardiac specification is unaltered in TBX5 and TBX20 morphants. Whole-mount in situ with *Nkx2.5* on stage matched (A,D,G,J) ControlMO-, (B,E,H,K) TBX5MO- or (C,F,I,L) TBX20MO-derived embryos.

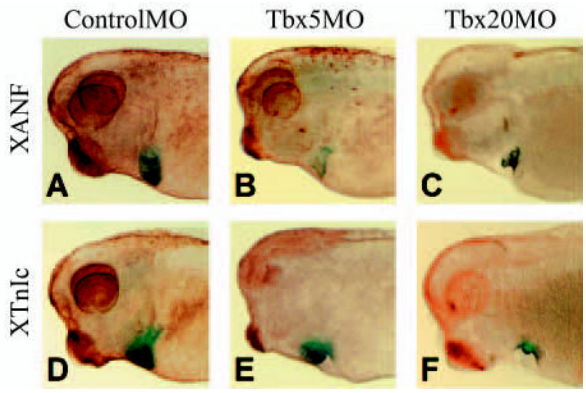

Fig. 5.

TBX5 and TBX20 morphants display dramatic morphological defects. Whole-mount in situ hybridization of cleared stage 36 embryos. (A–C) *ANF* whole-mount in situ hybridization. (D–F) *XTnIc* whole-mount in situ hybridization. (A,D) ControlMO. (B,E) TBX5MO and (C,F) TBX20MO.

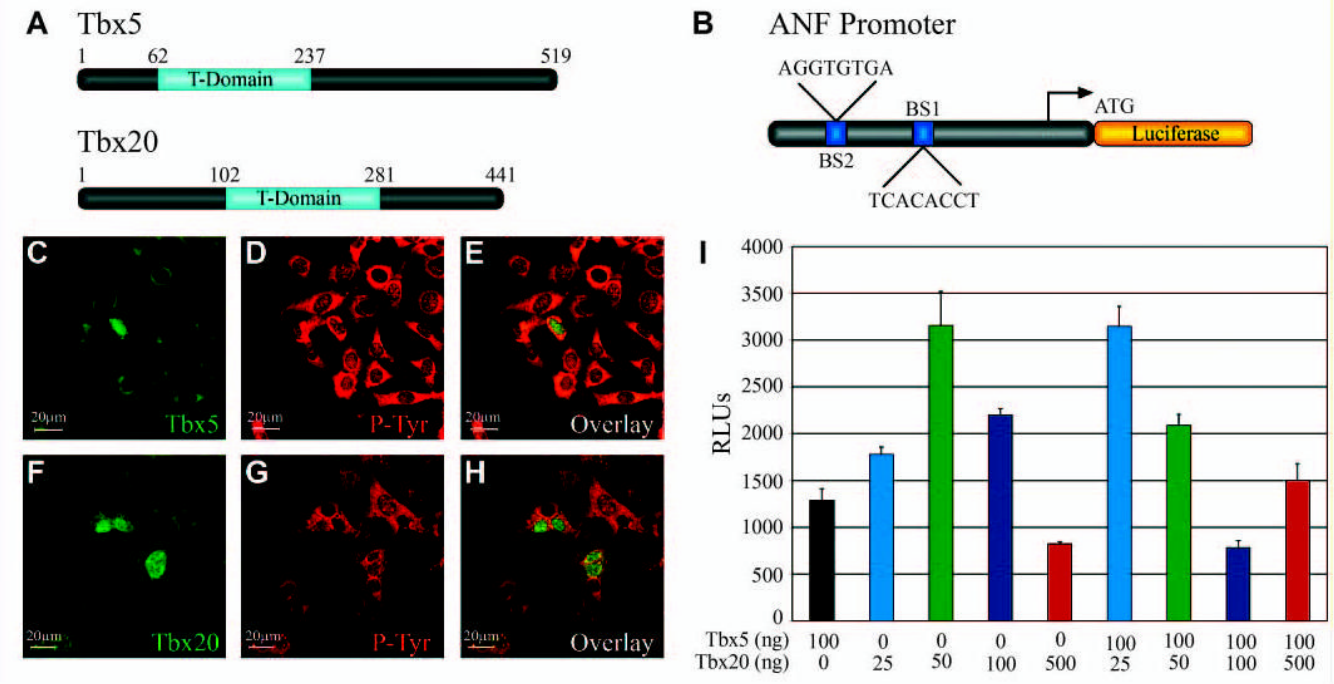

Fig. 6.

Tbx5 and *Tbx20* are localized to the nucleus and can activate transcription on the *Nppa*/*ANF* promoter. (A) Schematic depicting the amino acid positions of the T-box domains of *Tbx5* and *Tbx20*. (B) Schematic of Rat *Nppa*/*ANF-luciferase* reporter construct showing T-box-binding site consensus sequences and their relative position within the promoter relative to translation start site. (C–H) Transfected cells were stained with anti-V5 (C,F; Cy2, green) for TBX5-V5 and TBX20-V5, and with anti-phosphotyrosine (D,G; Cy3, red) to visualize cytoplasmic compartment. Overlaid image of Cy2 and Cy3 staining (E,H). (I) Rat *ANF-luciferase* co-transfected with a constant amount of *Tbx5* (100 ng) and increasing amounts of *Tbx20* (25, 50, 100 and 500 ng) in 293T cells, and the level of transcriptional activation is expressed as relative luciferase units based on average of three independent experiments performed in triplicate.

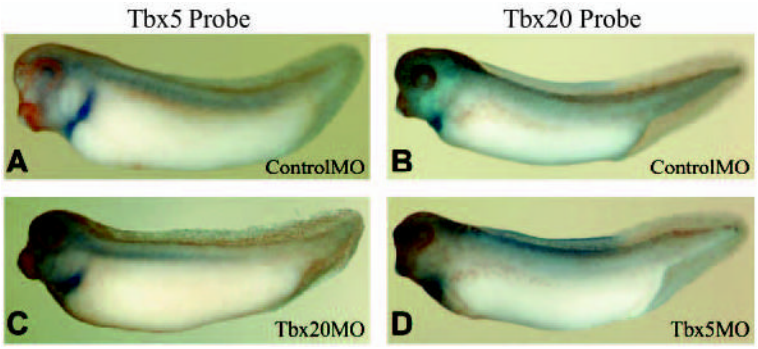

Fig. 7.

Tbx5 and *Tbx20* are not required for the expression of each other. Embryos injected at the one-cell stage with ControlMO, TBX5MO or TBX20MO. (A,C) Whole-mount in situ hybridization showing *Tbx5* expression. (B,D) Whole-mount in situ hybridization showing *Tbx20* expression.

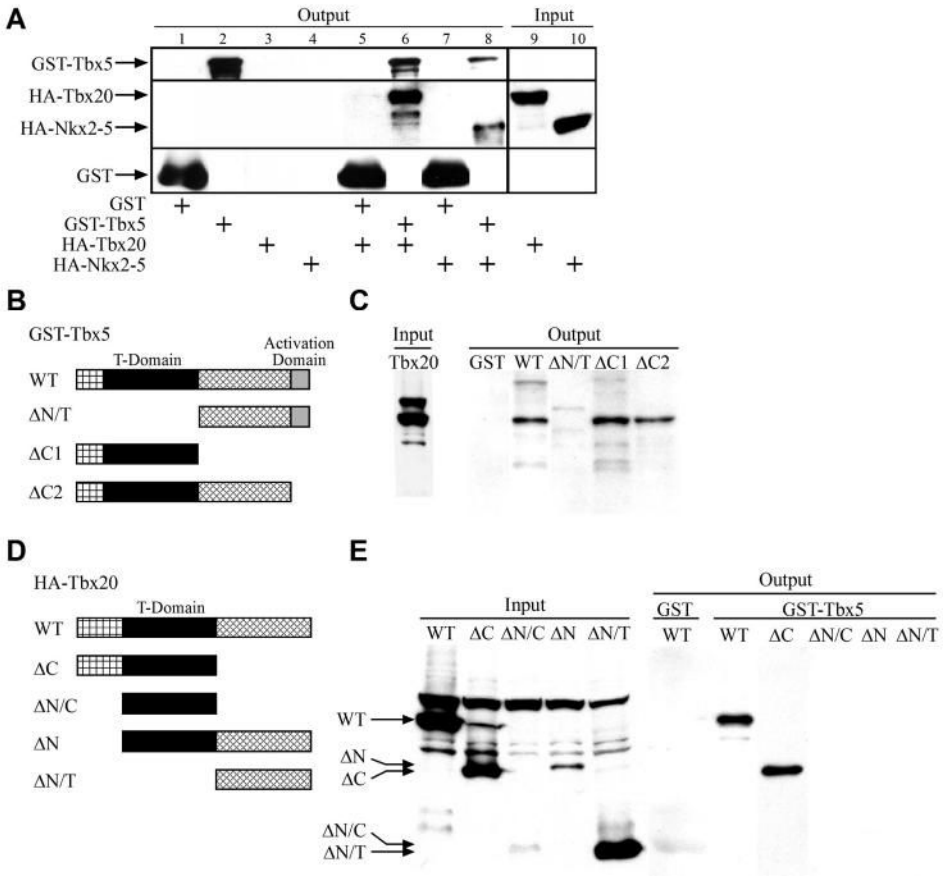

Fig. 8.

TBX5 and TBX20 physically interact. Cell lysates containing GST- and/or HA-tagged proteins were incubated on GST and eluted, and separated by SDS-PAGE. GST proteins were detected using anti-GST antibodies and HA-tagged proteins were detected with anti-HA antibodies. (A) Association of TBX5 with TBX20 is shown by pull-down of HA-TBX20 with GST-TBX5. HA-NKX2-5 serves as positive control. Fifteen percent of output and 7.5% of input was probed. (B,C) Pull-down of full-length HA-TBX20 with a GST-tagged TBX5 deletion series reveals an interaction domain in the N terminus and T-box region of TBX5. Each reaction was probed with anti-HA antibodies (B). Fifteen percent of output and 7.5% of input was probed. (D,E) Pull-down of HA-TBX20 deletion series with full-length GST-TBX5 reveals an interaction domain within the N-terminus and T-box of TBX20. Each reaction was probed with anti-HA antibodies (D). Fifteen percent of output and 7.5% of input was probed, except in the case of ΔN/C, in which the amount of protein probed was only 4% owing to the increase in total amount of ΔN/C protein used in pull-down (see text).

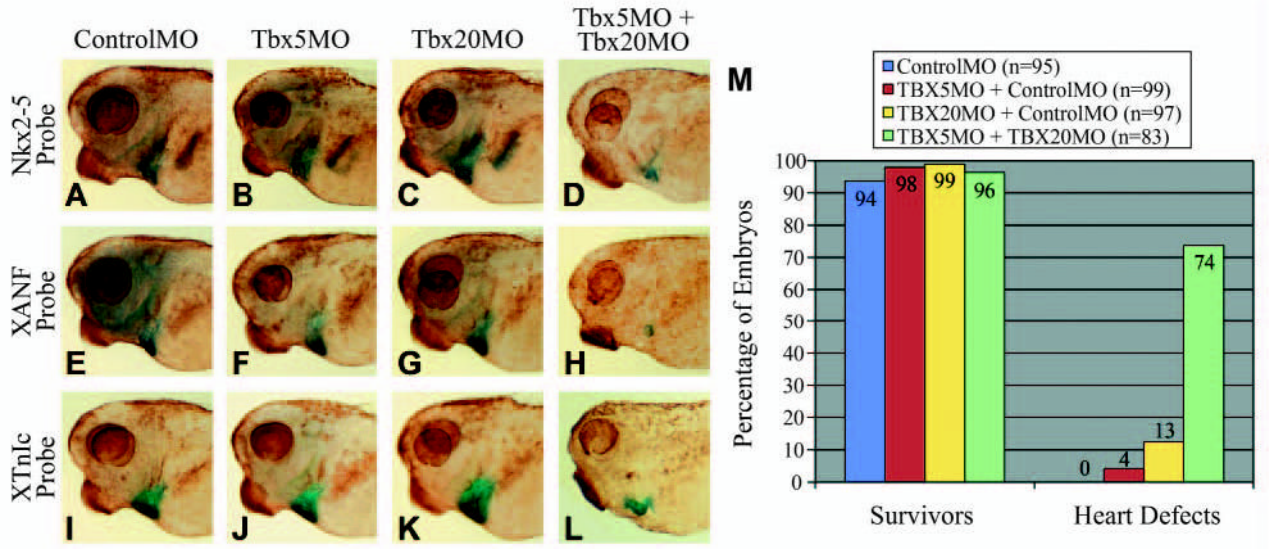

Fig. 9.

Tbx5 and *Tbx20* synergistically act to regulate cardiac gene expression. (A–L) Embryos injected with the indicated morpholinos at the one-cell stage. (A–D) *Nkx2-5* whole-mount in situ hybridization. (E–H) *XANF* whole-mount in situ hybridization. (I–L) *XTnIc* whole-mount in situ hybridization. (A,E,I) ControlMO, (B,F,J) TBX5MO injected at suboptimal dose, (C,G,K) TBX20MO injected at suboptimal dose, (D,H,L) TBX5MO and TBX20MO injected in combination at suboptimal doses. All embryo were cleared to reveal heart expression. (M) Statistics for embryos injected with suboptimal doses of TBX5MO and TBX20MO in combination with each other or with ControlMO. Hearts were judged as having defects if they displayed a pericardial edema, an unlooped heart tube or reduction in cardiac mass.